FREE for Reading & Publication

Diamond Open Access

Local Fluctuations of Transformation to "Amorphous Diamond" from C$_{60}$ Fullerenes and Neutron-irradiated Graphite under Shock-compression

Keisuke Niwase*

Department of Physics, Hyogo University of Teacher Education, Kato, Hyogo 673-1494, Japan

*Corresponding author: E-mail: niwase@hyogo-u.ac.jp; Tel.: (+81) 795 44 2210

C$_{60}$ fullerene and neutron-irradiated graphite have been reported to directly transform into "amorphous diamond" under shock compression, but the transformation mechanism is still not clear. Here, we report local fluctuations in the transformation to "amorphous diamond" from C$_{60}$ fullerene and neutron- irradiated highly oriented pyrolytic graphite shock-compressed at 52 and 51 GPa respectively. For the platelets recovered from C$_{60}$ fullerene film after the shock-compression, we observed a small Raman peak of diamond, of which peak shape changes depending on the area of platelets. Peak fitting revealed that the diamond Raman peak shifts to lower frequency with increasing the peak width and decreasing the peak intensity. This corresponds to the decrease of the crystalline size of nano-crystalline diamond and indicates the existence of amorphous diamond at an area where the intensity of diamond peak vanished. For the recovered sample of neutron-irradiated highly oriented pyrolytic graphite, on the other hand, we found an appearance of domain boundary between optically transparent and opaque areas, which respectively correspond to transformed and untransformed areas, thereby suggesting some novel transformation process originated in the initial disordered structure.

Introduction

Synthesis of diamond from various carbon materials by physical or chemical routes is an interesting issue. Transparent nanocrystalline diamond, consisting of a few nanometer-sized diamond crystallites, were synthesized from C$_{60}$ fullerene films by shock compression and rapid quenching (SCARQ) technique [1-5]. Transmission electron microscopy and electron energy loss spectroscopy revealed that was modified sp^3 carbon nanometer-sized diamond crystallites [4]. Polycrystalline diamond has been synthesized also by direct conversion of graphite under static high pressure and temperature [6].

The ultimate smallest crystalline size of diamond was generated from C$_{60}$ fullerene films by shock compression and rapid quenching (SCARQ) technique [2-5]. The obtained material is comprised wholly of sp^3 carbon suggesting diamond structure, but the diamond crystalline size is within the range of a unit cell. Then it was labelled "amorphous diamond" as it is amorphous in the long- range order and diamond in the short-range order.

Direct transformation from graphite to "amorphous diamond" was firstly succeeded by using neutron-irradiated highly oriented pyrolytic graphite (HOPG) as a starting material by SCARQ [7-9]. High energy-resolution electron energy-loss spectroscopy and Soft-X-ray emission spectroscopy (SXES) measurements were performed for the amorphous diamond. From the onset energies of the K-shell excitation and the SXES spectra, the band gap energy of amorphous diamond was estimated to be 4 eV [9], which is smaller than that the value of crystalline diamond (5.5 eV). Recently, by using a diamond anvil cell (DAC) coupled with in situ laser heating, amorphous diamond was synthesized also from glassy carbon as a starting material [10].

On the transformation of graphite to diamond, martensitic and diffusive processes have been considered to occur [11-16]. Martensitic transformation may occur if pressure is applied perpendicular to the graphitic basal plane, although a small amount of shear stress is necessary to induce shear motion between the phases. A reconstructive, topotactic transformation mechanism has been also proposed for the discovery of nano-sized grains of interstratified graphite and diamond from Gujba, an extraterrestrially shocked meteorite [17].

The purpose of the present study is to give some insights on the transformation process to "amorphous diamond" under shock compression from the starting materials of C$_{60}$ fullerene and neutron irradiated highly oriented pyrolytic graphite, by investigating the local fluctuations on the transformation.

Experimental

We used C$_{60}$ fullerene purified to 99.9 % and neutron-irradiated highly oriented pyrolytic graphite of HOPG-ZYA as a starting material. Neutron irradiation was done at about 333 K to a dose of 2.6 x 10^{24} n m^{-2} (E> 1 MeV) in JAERI JRR-2 nuclear reactor. Displacement per atom

(DPA) for the neutron-irradiated specimen is estimated to be about 0.2 dpa [18].

Thin films were prepared by vacuum evaporation on gold disks for C_{60} fullerene [5] and by cleavage with a razor for the neutron-irradiated HOPG [7]. Gold disks of 12 mm in diameter were utilized for rapid quenching after shock-compression. Specimens inserted into capsules were subjected to shock loading from a flyer accelerated by a powder gun. C_{60} fullerene films and neutron-irradiated graphite films were shock compressed to 52 and 51 GPa [5,7], respectively. The samples recovered from the capsules were investigated by optical microscopy, and micro-Raman spectroscopy. Raman spectra were obtained with 488 nm light from an Ar-ion laser, focusing on the sample with a beam diameter of 2 μm and a power of 20 mW.
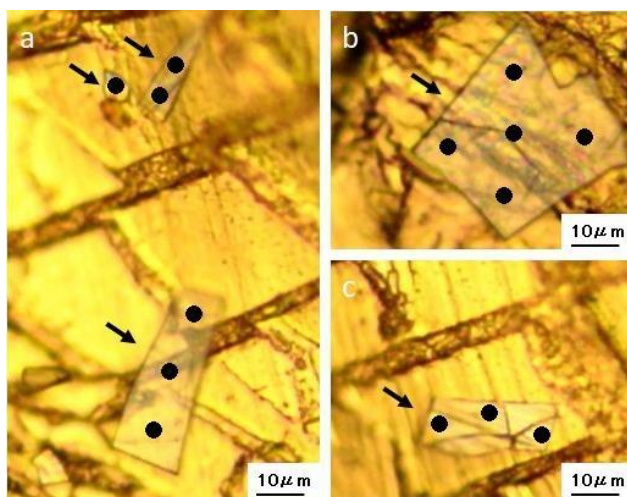

Fig. 1. Optical micrographs of platelets recovered from the starting material of C_{60} fullerene films after the shock compression and rapid quenching at 52 GPa. Platelets denoted by arrows are seen to be transparent. Filled circles show the areas, observed by micro-Raman spectroscopy. Trace of platelets can be seen on the surface of gold foil.

Results and discussion

C_{60} fullerene

After the shock compression of the evaporated C_{60} fullerene films at 52 GPa, we observed division of the recovered sample, indicating an occurrence of fracture into platelets [5]. The size of platelets ranged from several μm to several tens of μm. **Fig. 1** shows an optical micrograph of platelets on a gold foil. The platelets are seen to be transparent, as reported before [1-4]. Observations with micro-Raman spectroscopy were done for 26 areas of 8 platelets, as the areas were denoted by filled circles for the five platelets in **Fig. 1**. Four different Raman spectra obtained from the platelets are shown in **Fig. 2**. All the Raman spectra are seen to incline upward to the right. The inclination of the base line is not due a noise but due to photoluminescence which should originate in the disordered structure with sp³ bonding, as the photoluminescence appeared also after the shock compression of the neutron-irradiated HOPG

specimen [7]. In the spectra denoted by **b**, **c** and **d**, we can find a single peak near the position of diamond peak of 1333 cm⁻¹ indicating the formation of diamond crystal by the shock compression. Peak fittings were done for the Raman spectra obtained from the 8 platelets. We used a single Lorenzian peak and a baseline selecting a narrow range, as shown in **Fig. 3** for example.
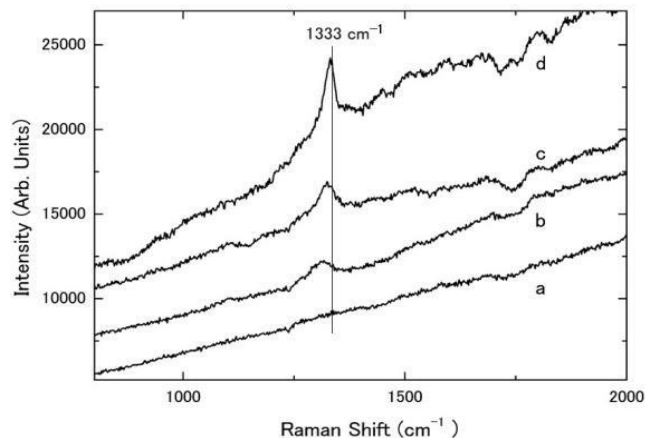

Fig. 2. Raman spectra for the different areas of platelets, which were recovered after the shock compression of C_{60} fullerene films at 52 GPa. Small diamond peak can be seen in the spectra denoted by **b**, **c** and **d**. The peak shape is seen to change depending on the platelets or the area of the platelets. The diamond peak cannot be seen in the spectrum denoted by **a**.
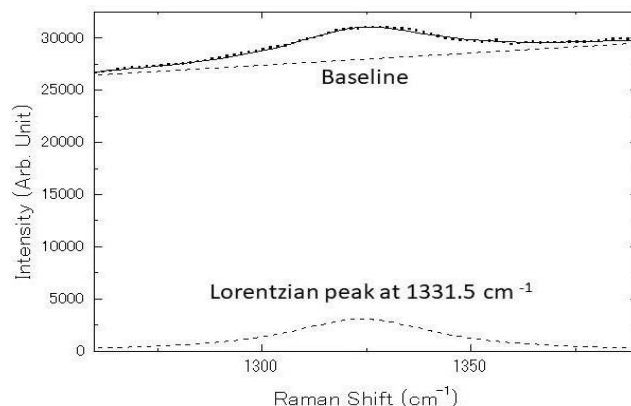
Fig. 3. An example of peak fitting for the Raman spectra obtained from the 8 platelets. We used a single Lorenzian peak and a baseline selecting a narrow range of the spectrum.

Figs. 4(a) and **4(b)** show the changes of the peak width (FWHM) and the peak intensity against the peak position, respectively, given by the fitting analyses. The position of the diamond Raman peak is seen to shift to lower frequency with increasing the peak width and decreasing the peak intensity. A similar downshift of the Raman peak has been reported for nano-crystalline diamond film, prepared by a conventional hot-filament chemical vapor deposition system in a CH_4/H_2 mixture [19]. With decreasing the particle size from 120 to 28 nm, the diamond peak shifts from 1332.8 to 1329.6 cm⁻¹, the line width of the peak becomes broader, and the intensity ratio of diamond against the graphite peak decreases. The result was explained by the phonon confinement model [20].
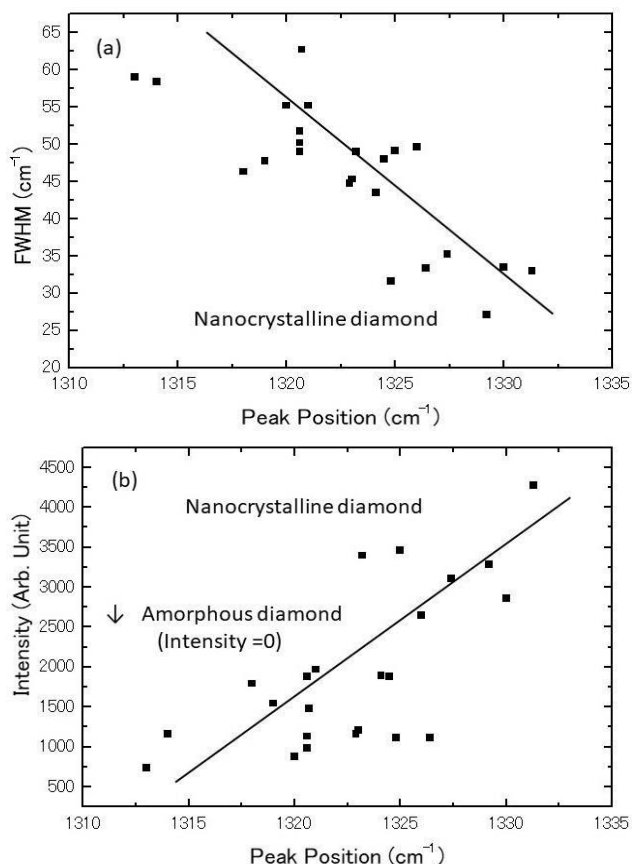
Fig. 4. The changes of (a) peak width (FWHM) and (b) Raman intensity of diamond peak against the peak position for the platelets recovered after the shock compression of C$_{60}$ fullerene films at 52 GPa. All the data were given by the fitting analysis given in Fig. 3. The diamond Raman peak is seen to shift to lower frequency with increasing the peak width and decreasing the peak intensity. Amorphous diamond should exist in the area where the diamond peak intensity becomes zero, as indicated in **Fig. 4b**.

The similarity between the present results and nano-crystalline diamond film, prepared by a conventional hot-filament chemical vapor deposition system, on the behaviour of the Raman spectral changes against the crystalline size of diamond [**19**] suggests that there exists fluctuation in the crystalline size, depending the part of the platelets in the recovered samples shown in **Fig. 5**. Judging from the significant down shift of the peak position, the crystalline size on the nano-crystalline diamond obtained in the present study can be smaller than the crystalline size of 28 nm which is the smallest one given for the vapour deposition system [**19**]. Moreover, the above consideration suggests the existence of amorphous diamond at the area where the Raman intensity of the diamond peak becomes zero, as seen for the spectrum **a** in Fig. 2.

Thus, the present finding on the change of the shape of diamond peak indicates the existence of local fluctuations in the crystalline size of nano-diamond, synthesized from the starting material of C$_{60}$ fullerene by the shock compression. Moreover, the fluctuation of the crystalline size against the areas of the recovered specimen suggests the nucleation and growth mechanism controlled by diffusion process on the formation.
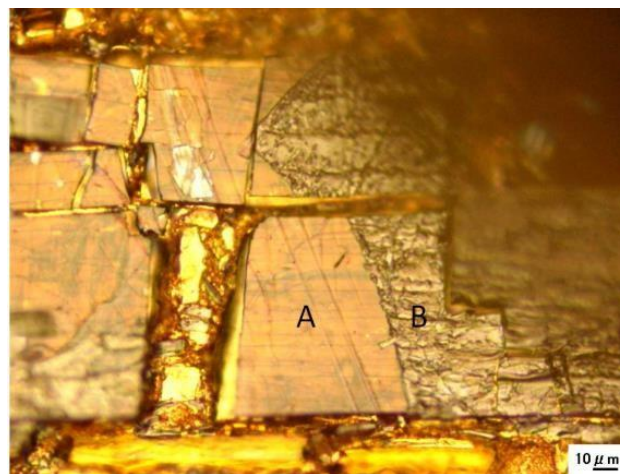
Fig. 5. A part of recovered sample of neutron-irradiated HOPG, which was shock-compressed at 51 GPa. One should note that there exist boundaries, dividing into two different areas, of which images denoted by **A** and **B** are transparent and opaque, respectively.

Neutron-irradiated graphite

Fig. 5 shows a part of recovered sample of neutron-irradiated HOPG, which was shock-compressed at 52 GPa. One should note that there exist boundaries, dividing into two different areas, of which images denoted by **A** and **B** are transparent and opaque, respectively. **Fig. 6** compares the Raman spectra for the area **A** and **B** of the shock-compressed HOPG shown in **Fig. 5**, and the original HOPG. Raman measurements were done in the same condition to compare the relative intensity. The original HOPG specimen shows a sharp graphite peak at 1580 cm^{-1} on E$_{2g}$ mode. After the neutron irradiation, the graphite peak disappeared, and then a broad band appeared [**7**], similarly to the case of ion irradiations [**21,22**]. The Raman shape is a broad one of amorphous carbon consisting mostly of sp^2 bonding [**23**].

After the shock compression, a remarkable increase in the background intensity appeared in the Raman spectrum obtained in the area **A** in **Fig. 5**. The spectrum exhibited a broad band at about 1600 cm^{-1}. In spite of the transparency, we cannot find the diamond peak at around 1333 cm^{-1}. The increase of the background intensity has also seen for the "amorphous diamond" synthesized from C$_{60}$ fullerene by the shock compression as described before, and is due to photo luminescence, probably originating in an existence of defective sp^3 bonding. The broad band at about 1600 cm^{-1} did not appear for the "amorphous diamond" synthesized from C$_{60}$ fullerene but did for the polymerized C$_{60}$ fullerene formed by a lower shock pressure [**5**]. This suggests that the transition to "amorphous diamond" is not complete in this case, remaining some sp^2 bonding.

In spite of the remarkable change of the Raman spectrum in the area **A**, the shape of Raman spectra in the area **B** still remained the broad one of neutron-irradiated HOPG with no photoluminescence [**7**]. This indicates that the transformation did not occur in the area **B**. One should note that there appeared clear boundaries, suggesting the

transformation process is not diffusive. Also, martensitic or a reconstructive, topotactic transformation processes are not likely, because the starting material of neutron-irradiated graphite is in highly a disordered state [**21,22**]. Thus, some novel transformation process should occur in the case of neutron-irradiated HOPG.

Recently, amorphous diamond was synthesized from glassy carbon as a starting material [**10**]. Ab initio MD simulation was shown as a possibility on the formation of amorphous diamond, by quenching from liquid carbon very slowly under high pressure, followed by pressure release to zero pressure [**10**]. The result indicates the random carbon structure like liquid can form a random structure, consisting mostly of sp^3 bonding.

In the present study, we used neutron-irradiated HOPG as the starting material, which possesses a unique structure of layered and highly disordered graphene planes, which can be cleaved. The appearance of clear boundary after the shock compression in **Fig. 5** may suggest an occurrence of cooperative transformation, in which the formation of sp^3 bonding can be enhanced by the formation of sp^3 bonding in the vicinity, as the formation of sp^3 bonding should makes the distance of the neighbouring planes shorter. The appearance of a broad peak near 1600 cm^{-1} and photoluminescence in the spectrum **A** in **Fig. 6** suggest remaining highly disordered structure with sp^2 and sp^3 bondings. Recent investigations on the transformation of the neutron-irradiated HOPG to the polycrystalline diamond [**24**] and the compressed graphite [**25**] under the static pressure may give some insights on the transformation process. Further experimental and theoretical works are awaited.
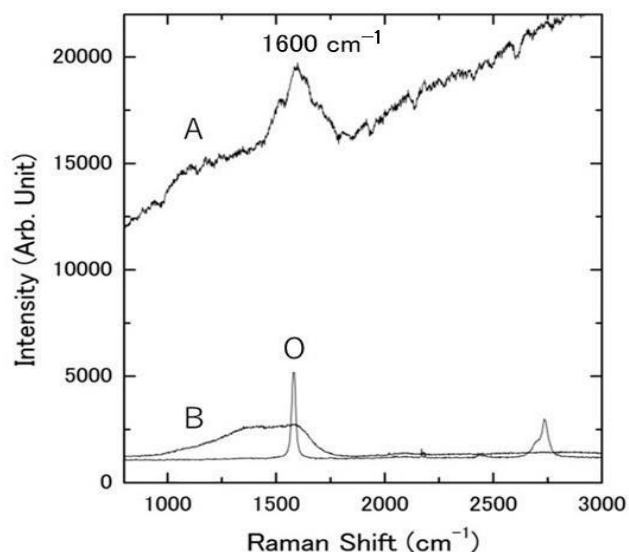
Fig. 6. Raman spectra for the neutron-irradiated HOPG specimen after the shock compression at 51 GPa and for the original HOPG. Spectrum on the original HOPG denoted by **O** shows the first-order band (G band) near 1580 cm^{-1} and the second-order Raman band near 2700 cm^{-1}. Spectrum **A** on the shocked specimen obtained in the area denoted by **A** in **Fig. 5** shows a significant increase of the background intensity and an appearance of a broad band near 1600 cm^{-1}. The spectrum **B** obtained in the area denoted by **B** in **Fig. 5**, on the other hand, shows almost no change from the original broad band after the neutron irradiation.

Conclusion

We synthesized "amorphous diamond" from C_{60} fullerene and neutron-irradiated highly oriented pyrolytic graphite by shock-compression, and investigated local fluctuation on the transformation to give some insight on the transformation process. A small Raman peak of diamond was observed with a background of photoluminescence for the platelets recovered from a C_{60} fullerene film after shock-compression at 52 GPa. We found local fluctuation on the shape of the small diamond peak; the peak shifts from 1309 to 1332 cm^{-1} with decreasing the peak width and increasing the peak intensity. This indicates a gradual increase in the crystalline size, suggesting diffusive process on the nucleation and growth of nano-diamond. The recovered sample of neutron-irradiated graphite after shock-compression at 51 GPa, on the other hand, exhibited an appearance of a domain boundary between optically transparent and opaque areas. Raman spectroscopy revealed that the transparent and the opaque areas correspond to transformed and untransformed areas, suggesting some novel transformation process to the "amorphous diamond", which can occur in the highly disordered structure of neutron-irradiated graphite.

References

1. Yoo, C.S.; Nellis, W.J.; Sattler, M.L.; Musket, R.G.; *Appl. Phys. Lett.* **1992**, 61, 273.
2. Hirai, H.; Kondo, K.; Yoshizawa, N.; Shiraishi, M.; *Appl. Phys. Lett.* **1994**, 64, 1797.
3. Hirai, H.; Tabira, Y.; Kondo, K.; Oikawa, T.; Ishizawa, N.; *Phys. Rev. B*, **1995**, 52, 6162.
4. Hirai, H.; Kondo, K.; Kim, M; Koinuma, K.; Kurashima, K.; Bando, Y.; *Appl. Phys. Lett.* **1997**, 71, 3016.
5. Niwase, K.; Homae, T.; Nakamura, K.G.; Kondo, K.; *Physica B*, **2006**, 376-377, 280.
6. Irifune, T.; Kurio, A.; Sakamoto, S.; Inoue, T.; Sumiya, H. ; *Nature* **2003**, 421, 599.
7. Niwase, K.; Nakamura, K.G.; Yokoo, M.; Kondo, K.; Iwata, T.; *Phys. Rev. Lett.*, **2009**, 102, 116803.
8. Niwase, K.; Atou, T.; Nakamura, K.G.; Iwata, T.; *J. Phys.Condence. Matter*, **2012**, 377, 012026.
9. Sato, Y.; Terauchi, M.; Niwase, K.; Nakamura, K. G.; Atou, T.; Iwata, T.; *J. Phys. Conf. Ser.*, **2014**, 500, 192013.
10. Zeng, Z.; Yang, L.; Zeng, Q.; Lou, H.; Sheng, H.; Wen, J.; Miller, D.J.; Meng, Y.; Yang, W.; Mao, W.L.; Mao, H.; *Nat. Commun.*; **2017**, 8, 322.
11. Erskine, D.J.; Nellis, W. J.; *Nature*, **1991**, 349, 317.
12. Erskine, D.J., Nellis, W. J.; *J. Appl. Phys.*, **1992**, 71, 4882.
13. Tateyama, Y.; Ogitsu, T.; Kusakabe, K.; Tsuneyuki, S.; *Phys. Rev. B*, **1996**, 54, 14994.
14. Sumiya, H.; Irifune, T.; Kurio, A.; Sakamoto, S.; Inoue, T.; *J. Mater. Sci.*, **2004**, 39, 445.

15. Ohfuji, H.; Okimoto, S.; Kunimoto, T.; Isobe, F.; Sumiya, H. Komatsu, K.; Irifune, T.; *Phys. Chem. Minerals*, **2012**, 39, 543– 552.
16. Isobe, F.; Ohfuji, H.; Sumiya, H.; Irifune, T.; *J. Nanomater.*, **2013**, Article ID 380165, 6 pages.
17. Garvie, L.A.J.; Nemeth, P.; Buseck, P.R.,; *Am. Min.*, **2014**, 99, 531.
18. Iwata, T.; Nihira, T.; J. *Phys. Soc. Jpn.*, **1971**, 31, 1761.
19. Sun, Z.; Shi, J.R.; Tay, B.K.; Lau, S.P.; *Diam. Relat. Mater.*, **2000**, 9 , 1979.
20. Nakamura, K.G.; Fujitsuka, M.; Kitajima, M.; *Phys. Rev. B*, **1990**, 41, 12260.
21. Niwase, K.; *Phys. Rev. B*, **1995**, 52, 15785; *Phys. Rev. B*, **1997**, 56, 5685.
22. Niwase, K.; *Int. J. Spectrosc.*, **2012**, 2012, 197609.
23. Ferrari, A. C.; Robertson, J., *Phil. Trans. R. Soc. London. A*, **2004**, 362, 2477.
24. Terasawa, M.; Honda, S.; Niwase.; K.; Niibe, M.; Hisakuni, T.; Iwata, T.; Higo, Y.; Hirai, T.; Shinmei, T.; Ohfuji, H.; Irifune, T.; *Diam. Relat. Mater.*, **2018**, 82, 132-136
25. Niwase.; K.; Terasawa, M.; Honda, S.; Niibe, M.; Hisakuni, T.; Iwata, T.; Higo, Y.; Shinmei, T.; Ohfuji, H.; Irifune, T.; *J. Appl. Phys.*, **2018**, 123, 161577.